Treatment of Tebuthiuron in synthetic and real wastewater using electrochemical flow-by reactor

Aline J. M. da Costa, Matheus S. Kronka, Paulo J. M. Cordeiro-Junior, Guilherme V. Fortunato, Alexsandro J. dos Santos*, Marcos R. V. Lanza*

São Carlos Institute of Chemistry, University of São Paulo, Avenida Trabalhador São-Carlense 400, São Carlos, SP, 13566-590, Brazil.

*Corresponding author's e-mail:

alexsandrojhones@usp.br (A. J. dos Santos)

marcoslanza@usp.br (M. R. V. Lanza)

Abstract

The inefficiency of conventional water treatment methods in the treatment of recalcitrant herbicides has led to the search for new, efficient and eco-friendly mechanisms for degrading these organic pollutants. Electrochemical advanced oxidation processes (EAOP) have emerged as a promising alternative due to their high degree of efficiency in degrading organic pollutants. This work investigates the removal of Tebuthiuron (TBH) in synthetic and real wastewater using different EAOPs in a flow-by reactor. The degradation/mineralization experiments were performed using boron-doped diamond electrode as anode and gas-diffusion electrode (GDE) as cathode for the *in situ* electrogeneration of hydrogen peroxide (H_2O_2). For the analysis conducted in synthetic medium, TBH degradation was found to fit well in a pseudo-first-order kinetic reaction with increasing k_1 values according to the following order of efficiency: anodic oxidation (AO, $3.1x10^{-5}$ s^{-1}) < AO with H_2O_2 generation (AO-H_2O_2, $4.8x10^{-5}$ s^{-1}) < electro-Fenton (EF, $5.9x10^{-5}$ s^{-1}) < AO-H_2O_2/UVC ($2.6x10^{-4}$ s^{-1}) < photoelectro-Fenton (PEF, $3.2x10^{-4}$ s^{-1}). AO-H_2O_2/UVC and PEF processes presented the highest rates of mineralization and similar energy consumption per order (~ 45 kWh m^{-3} $order^{-1}$). The degradation experiment conducted using real urban wastewater yielded a 1.7-fold decrease in TBH degradation kinetics compared to the synthetic medium; this difference was attributed to the presence of inorganic ions and natural organic matter in real wastewater which tended to affect the electrochemical system efficiency. The findings of this study are of great interest and confirm the viability of electrochemical techniques for treating complex effluents contaminated by herbicides.

Keywords: H_2O_2 electrogeneration, electrochemical advanced oxidation processes, Tebuthiuron, real wastewater treatment, flow-by reactor.

1 Introduction

Between 1990 and 2018, Brazil was ranked third (~221 tons per year) among the highest consumers of pesticides in the world [1]. A recent survey revealed that herbicides account for more than 60% of Brazil's total pesticides consumption [2]. The huge consumption of pesticides in the country is primarily related to the fact that Brazil is one of the leading producers of coffee, orange, corn, sugarcane and soybean in the world. Sugarcane and soybean cultivations are widely known to be seriously affected by weeds; and one of the efficient ways of tackling this problem involves the application of a broad spectrum herbicide such as the 1-(5-tert-butyl-1,3,4-thiadiazol-2-yl)-1,3-dimethylurea, commercially known as Tebuthiuron (TBH), which belongs to the class of phenyl urea [3–6]. However, studies published in the literature have shown that TBH has low absorption rate in the soil and it is extremely persistent in water bodies, in addition to exhibiting high degree of resistance to chemical and biological degradation techniques and high rate of toxicity to the aquatic biota [3–7]. These findings have raised serious concerns among researchers regarding the widespread use of TBH for weed control and its rampant disposal in the environment and have boosted the search for efficient degradation mechanisms for the treatment of TBH in wastewater. In this context, traditional treatment methods have been applied in an effort to degrade TBH in wastewater and in other water bodies. Owing to its recalcitrant characteristics, other alternative processes, such as electrochemical advanced oxidation processes (EAOP), which are mainly employed for the treatment of persistent compounds in environmental effluents, have also been successfully tested aiming at the degradation of TBH [8–14].

EAOPs are based on *in-situ* generation of reactive oxygen species such as hydroxyl radical ($^{\bullet}OH$); this radical is a strong oxidant ($E^{o}(^{\bullet}OH/H_2O)$ = 2.8 V/SHE at pH 0) which has been shown to be capable of degrading and mineralizing a wide range

of toxic and persistent organic pollutants[15,16]. Among the EAOPs, anodic oxidation (AO) has been widely employed for the treatment of pollutants because of its simplicity and high efficiency [17,18]. The efficiency of AO largely depends on the type of anodic material employed. The underlying fundamentals and principles regarding AO and its application have been extensively described in the literature [19–23]. The AO process can be conducted in the presence of electrogenerated hydrogen peroxide (H_2O_2); this approach, denoted here by AO-H_2O_2, allows the removal of contaminants mainly by the attack of heterogeneous $^{\bullet}OH$ on the anode surface after water electrolysis (Eq. 1) [24–26]. Under the AO-H_2O_2 process, H_2O_2 can be continuously generated from the two-electron reduction of injected oxygen gas on carbonaceous cathodes (Eq.2) such as graphite, carbon sponge, carbon felt, carbon black, carbon nanotubes, and carbon-poly(tetrafluoroethylene) composite (PTFE) [27–33]. The efficiency of the AO-H_2O_2 process can be enhanced via the activation of the electrogenerated H_2O_2 by Fe^{2+} (electro-Fenton) (Eq. 3) and/or in the presence of UV-C radiation (Eq. 4), leading to the generation of homogeneous $^{\bullet}OH$ [34–36].

$$H_2O \rightarrow {}^{\bullet}OH + H^+ + e- \quad \text{(Eq. 1)}$$

$$O_2 + 2H^+ + 2e^- \rightarrow H_2O_2 \quad \text{(Eq. 2)}$$

$$Fe^{+2} + H_2O_2 \rightarrow Fe^{+3} + OH^- + {}^{\bullet}OH \quad \text{(Eq. 3)}$$

$$H_2O_2 + h\nu \rightarrow 2\ {}^{\bullet}OH \quad \text{(Eq. 4)}$$

Most of the works that have been published in the literature regarding TBH removal by EAOPs [8,37–40] were conducted using an electrochemical lab-scale apparatus with ultrapure water. The treatment of pollutants present in real effluents in scaled-up systems is a major challenge since the coexistence of different species in real water matrices can affect the electrochemical treatment technique [41,42]. In the present work, the treatment of TBH was conducted by mimicking a water sample containing a

known amount of commercial TBH using different EAOPs in a flow-by reactor. Studies were conducted to assess the performance of the system in terms of H_2O_2 electrogeneration, pollutant removal, and electrical energy per order. Inorganic by-products, such as sulfate, nitrite and chloro-oxyanions present in the real water matrix and from degradation of THB were quantified. Finally, the viability of the electrochemical techniques was put to test by depurating real urban wastewater containing TBH.

2 Experimental

2.1 Chemicals

TBH ($C_9H_{16}N_4OS$ MW = 228.31 g mol^{-1}) with 99% purity, acquired from Supelco (Sigma-Aldrich), was used for constructing the analytical curve for HPLC and the commercial TBH (Combine 500 SC - Dow AgroSciences Industrial Ltda., Brazil) was used for conducting the degradation experiments. The following compounds were used for performing the experiments: iron (II) sulfate heptahydrate ($FeSO_4.7H_2O$), sulfate potassium (K_2SO_4), sulfuric acid (H_2SO_4), ammonium molybdate ($(NH_4)_6Mo_7O_{24}$), acetonitrile (CH_3CN) (all with high purity, purchased from Vetec). Poly(tetrafluoroethylene) (PTFE) hydrophobic binder (60% aqueous dispersion) - purchased from Dupont (USA), was used in the experiments. Ultrapure water obtained from a Milli-Q system (resistivity >18 MΩ cm) was used for preparing all the solutions. All other reagents used for the experimental analyses were of analytical or HPLC grade (the reagents were acquired from Sigma-Aldrich).

2.2 Electrochemical assays

The experiments were carried out in a flow-by reactor, operating as shown in Figure 1. The analytical solutions flowed through the reaction system, starting from the

115 tank (with a capacity of ~2.0 L) and moving to the electrochemical cell, then to the UV-
116 C light system, and moving back to the tank. The hydraulic pump supplied a flow of 50
117 L h^{-1}, which was controlled by a flow meter. The flow rate operated in a laminar flow
118 (Reynolds number of ~600) [43]. A boron-doped diamond (BDD) material and gas
119 diffusion electrode (GDE) were used as anode and cathode, respectively; the electrodes
120 covered a geometric area of 20 cm^2, with inter-electrode gap of 0.8 cm. The GDE was
121 prepared as described in refs. [43,44]. The catalytic mass used in the electrodes was
122 prepared by mixing carbon black (Printex L6 carbon from Evonik), which was
123 previously thermally activated for 24 h at 120 °C, with 40 % (w/w) of PTFE aqueous
124 dispersion. Before the electrolysis, the electrodes were polarized in 0.1 mol L^{-1} K_2SO_4
125 at current density of 75 mA cm^{-2} for 30 min in order to remove impurities from the
126 BDD surface and to activate the GDE.

127 The electrolysis was performed using a DC power supply FA-2030 coupled to
128 an ampere meter ITMDB 100 ampere and a voltmeter MDB-450 (all acquired from
129 Instrutherm). Different current densities (*j*, 10 to 125 mA cm^{-2}) were employed in order
130 to evaluate the accumulation of H_2O_2 in the reactor. Degradation experiments were
131 conducted using different EAOPs aiming at degrading 100 mg L^{-1} TBH in both
132 synthetic wastewater and real urban wastewater. The urban wastewater was collected
133 after aerobic / anaerobic bacterial treatment from a wastewater treatment plant (WWTP)
134 in the city of Bariri, São Paulo State (Brazil), and kept refrigerated at 4 ^{o}C. The main
135 characteristics of the effluent were summarized in table 1.

136 Photo-assisted experiments were carried out under ultraviolet irradiation using a
137 UV-C Hg lamp from PHILIPS (model: TUV 15/G15 T8) that provided 64 Wm^{-2} of
138 irradiance. For the EF and photo EF (PEF) processes, different concentrations of Fe^{2+}
139 (0.1, 0.25 and 1.0 mmol L^{-1}) were tested to determine the ideal quantity of this catalyst.

Table 1. Characteristics of the real urban wastewater.

pH	7.70
Conductivity	2.10 mS cm^{-1}
Total organic carbon	10.32 mg C L^{-1}
Ammonia	5.81 mg L^{-1}
Calcium	30.94 mg L^{-1}
Magnesium	6.07 mg L^{-1}
Potassium	15.54 mg L^{-1}
Sodium	90.68 mg L^{-1}
Chloride	53.62 mg L^{-1}
Nitrate	8.67 mg L^{-1}
Nitrite	0.98 mg L^{-1}
Sulfate	20.43 mg L^{-1}

2.3 Analytical techniques

The pH of the solutions was adjusted to ~ 3.0 using a pH-meter ION pHB500. The electrogenerated H_2O_2 was quantified by UV-Vis spectrophotometry (Shimadzu UV-1900), where 0.5 mL of the sample was placed in 4 mL of ammonium molybdate solution (2.4×10^{-3} mol L^{-1}). This approach was adopted due to the ability of molybdate to form a colored complex with H_2O_2 (which presents absorption band in the UV-Vis region at 350 nm) [45]. The percentage of current efficiency (CE) and the electric energy consumption (EC) were calculated using the H_2O_2 values and based on equations 5 and 6 below:

$$CE_{\mathrm{H_2O_2}}(\%) = \frac{2\ \mathrm{F}\ \mathrm{C_{H_2O_2}}\mathrm{V_s}}{I\ t} \times 100 \quad \text{(Eq. 5)}$$

$$EC\ (kWh\ kg^{-1}) = \frac{1000\ E\ I\ t}{V_S\ C_{H2O2}} \quad \text{(Eq. 6)}$$

where 2 corresponds to the number of electrons needed for the reduction of O_2 to H_2O_2, F is the Faraday constant (96,487 C mol^{-1}), C_{H2O2} is the H_2O_2 concentration (mol

L^{-1} for CE and mg L^{-1} for EC), V_s is the volume cell in L, I is the applied current in A, t is the electrolysis time (s for CE and h for EC), and E is the cell potential in V [46,47].

Degradation reactions were monitored by High Performance Liquid Chromatography (HPLC) using Shimadzu Prominence HPLC model LC-20 AT coupled to an SPD-20A UV detector at 249 nm. The separation was performed using a Varian C18 column (250 x 4.6 mm i.d., 5µm) and an isocratic mobile phase, which consisted of ultrapure water: acetonitrile (in the ratio 70:30%), with flow rate of 0.8 mL min^{-1} and retention time of 11.3 minutes for TBH. The oven temperature of 40 °C and injection volume of 20 µL were employed. The mineralization rate was monitored by total organic carbon (TOC) using Shimadzu TOC analyzer (model TOC-VCPN). All samples collected were filtered with a Chromafil Xtra PET 25 mm (diameter) x 0.45 µm (pore size) syringe filter before using them for the HPLC and TOC analyses. The percentages of TBH removal and TOC removal were calculated based on equations 7 and 8 below:

$$TBH\ removal\ (\%) = \frac{TBH_0 - TBH}{TBH_0}\ x\ 100 \quad \text{(Eq. 7)}$$

$$TOC\ removal\ (\%) = \frac{TOC_0 - TOC}{TOC_0}\ x\ 100 \quad \text{(Eq. 8)}$$

where TBH_0 and TOC_0 represent the concentration values of TBH and TOC at time 0, and TBH and TOC stand for the concentration values of TBH and TOC at a specific time t.

Inorganic species were detected with the aid of an Ion Chromatography system model 850 Professional IC ion chromatograph coupled to a 940 Professional IC module (Metrohm) with a 580 IC Conductimetric Detector. A sample of 20 µL was injected via an 863 Compact Autosampler. A Metrosep C4 column (150 mm/4.0 mm) and Metrosep C4 Guardian/4.0 pre-column were used for the determination of cations, while a Metrosep A Supp 5 column (150 mm/4.0 mm) and Metrosep A Supp 5 Guardian/4.0 pre-column were used for anions determination. The mobile phases employed were 1.7

mmol L^{-1} HNO_3/0.7 mmol L^{-1} dipicolinic acid solution and 3.2 mmol L^{-1} Na_2CO_3/1.0 mmol L^{-1} $NaHCO_3$, both applied at 0.90 and 0.70 mL min^{-1} for the analyses of cations and anions, respectively.

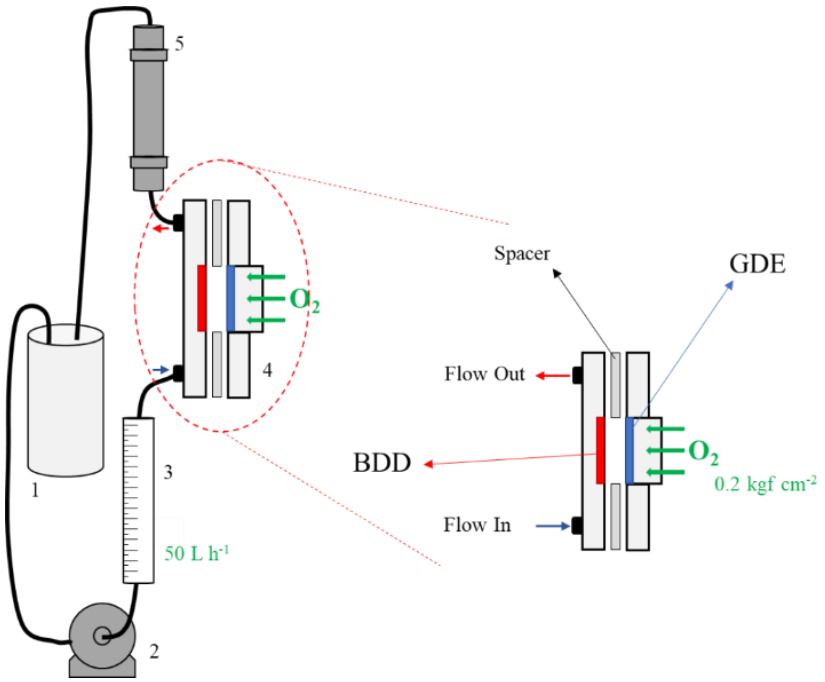

Figure 1. Illustrative scheme of the electrochemical flow-by reactor. The scheme shows the following: presence of ~ 2.0 L capacity tank (1), hydraulic pump (2), flow meter (3), electrochemical cell (4), and UV light compartment (5).

3 Results and discussion

3.1 H_2O_2 accumulation in the flow-by reactor

Different current densities (*j*) were tested in order to evaluate the ability of the reactor to generate and accumulate H_2O_2. To conduct this analysis, 0.1mol L^{-1} K_2SO_4 (with pH 3.0) was used as supporting electrolyte and the reactor temperature was kept constant at 25 ºC. As can be seen in Fig. 2, after 120 min of electrolysis, there was a gradual increase in H_2O_2 concentration over time with maximum concentrations of 87.8,

249.2, 484.4, 540.8 mg L^{-1} recorded for 10, 25, 50 and 75 mA cm^{-2} current densities, respectively. However, between 100 and 125 mA cm^{-2}, there was a decrease in the accumulation of the H_2O_2 from 327.5 and 187.2 mg L^{-1}.

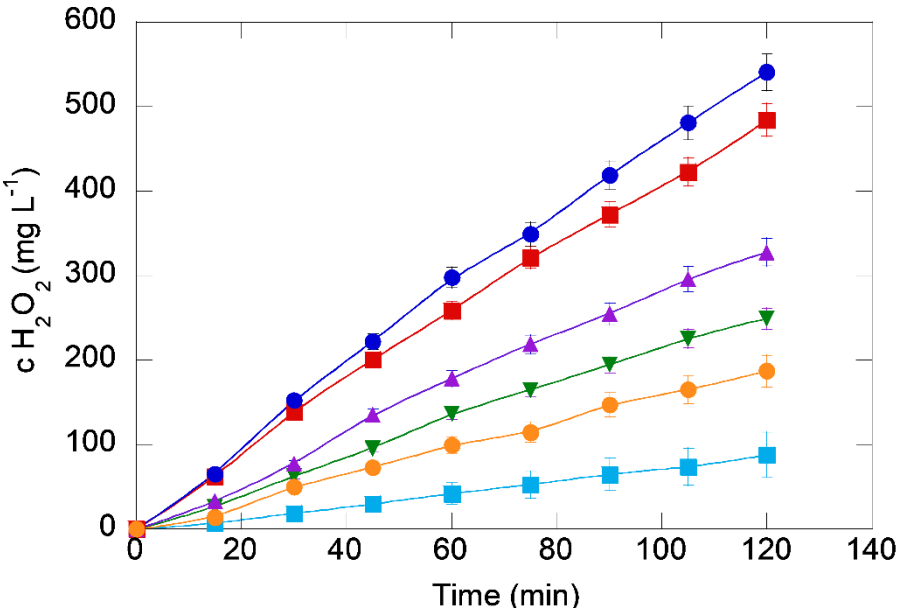

Figure 2. Quantity of H_2O_2 accumulated over time in a flow-by reactor at pH 3.0, with temperature of 25 ºC, based on the application of 0.1 mol L^{-1} K_2SO_4 under the following current densities: (■) 10 mA cm^{-2}, (▲) 25 mA cm^{-2}, (■) 50 mA cm^{-2}, (●) 75 mA cm^{-2}, (▼) 100 mA cm^{-2} and (●) 125 mA cm^{-2}.

In general, a greater H_2O_2 accumulation is expected as the current density *(j)* increases once a greater number of electrons will be available in the system. However, the progressive increase of *j* leads to a higher rate of parasitic reactions in the system. H_2O_2 is not inert in solution; it can be decomposed by oxidation on the surface of the BDD material (Eq. 9) and reduced to H_2O at the cathode (Eq. 10) [28,31].

$$BDD + H_2O_2 \rightarrow BDD(HO_2\bullet) + H^+ + e^- \quad \text{(Eq. 9)}$$

$$H_2O_2 + 2H^+ + 2e^- \rightarrow 2H_2O \quad \text{(Eq. 10)}$$

This behavior has been reported by other authors in studies involving the use of lab scale and pre-pilot plant setup [48–50]. The current efficiency data obtained corroborate this observation. As can be seen in Fig 3, the CE exhibited a quite constant behavior (62 - 70%) up to the current density of 50 mA cm^{-2}; however, after the current density of 75 mA cm^{-2}, the CE began to fall dramatically, recording the lowest value (of 10.67%) at 125 mA cm^{-2}. In contrast, the data related to energy consumption recorded a smooth rise to 34.7 kWh kg $H_2O_2^{-1}$ up to the current density of 100 mA cm^{-2} and an intense rise to 190.3 kW h at the current density of 125 mA cm^{-2}.

Despite the best current efficiency of H_2O_2 was observed at 50 mA cm^{-2}, the current density of 75 mA cm^{-2} was selected to be tested for TBH treatment, since it presented the best result in terms of H_2O_2 electrogeneration. It is worth noting that the current density *(j)* is an electrokinetic factor which controls the number of electrons available in the reactor; and even though a decrease in current efficiency is observed when this factor *(j)* increases from 50 to 75 mA cm^{-2} (see Fig 3), the presence of a greater number of oxidants at the anode (mostly heterogenous $^{\bullet}OH$) helps enhance the synergistic effect related to the pollutant removal.

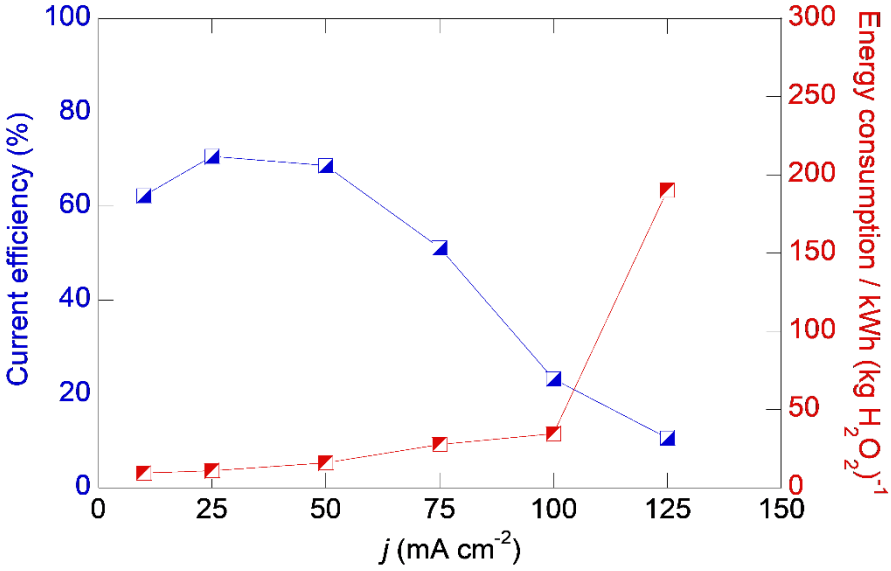

Figure 3. Current efficiency and energy consumption *vs.* different current densities for electrogeneration of H_2O_2.

3.2 TBH degradation and mineralization using EAOPs

For purposes of comparison, synthetic effluent containing 100 mg L^{-1} (48 mg L^{-1} TOC) of commercial TBH was subjected to treatment using different EAOPs with BDD anode and GDE cathode at 25 °C and pH 3.0 in a flow-by reactor. Figure 4a depicts the percentage of TBH removed over time; as can be noted in the figure, the pollutant was degraded in all the treatment processes employed. After 120 min of treatment, AO, AO-H_2O_2 and EF processes promoted 22.4%, 27.6% and 32.7% of TBH removal, respectively. Photo-assisted processes (AO-H_2O_2/UVC and PEF) presented almost total degradation under identical operating conditions. The removal of TBH fitted well in a pseudo-first-order kinetic model. The efficiency of the EAOPs investigated was compared in terms of TBH kinetics, TOC removal and energy consumption per order (Fig, 5a and 5b). Fig. 5a shows that the processes with lower TBH degradation kinetic constants also recorded lower TOC removal rates. The values related to k_1 and TOC removal increased in the following order: AO (3.1×10^{-5} s^{-1} – R^2=0.987, 11.4%), AO-

H_2O_2 ($4.8x10^{-5}s^{-1}$ – R^2=0.996, 12.3%), EF ($5.9x10^{-5}s^{-1}$ – R^2=0.989, 14.7%), AO-H_2O_2/UV ($2.6x10^{-4}$ s^{-1} – R^2=0.993, 21.8%) and PEF ($3.2x10^{-4}$ s^{-1} – R^2=0.991, 30.1%). An 8.1-fold increase was observed from the process with the lowest TBH removal to the highest. This behavior was found to be dependent on the oxidative power of each process. In the AO process (using BDD anode), water electrolysis promoted the generation of large amounts of physisorbed $^{\bullet}OH$ (Eq. 1), and this paved the way for TBH degradation. The application of the AO-H_2O_2 process led to the removal of the pollutant mainly by the attack of BDD($^{\bullet}OH$) radicals, and to a lesser extent, by the action of H_2O_2 and hydroperoxyl radical (Eq. 9, $HO_2^{\bullet}$), which are considered relatively weak oxidants [46].

The efficiency of the AO-H_2O_2 process was slightly improved by the incorporation of the homogeneous Fe^{2+} catalyst in the medium; this is attributed to the fact that the catalyst promotes the generation of homogeneous $^{\bullet}OH$ radicals from Fenton reaction (Eq. 3) and the continuous regeneration of Fe^{2+} by Fe^{3+} reduction at the cathode [24,51]. It is noteworthy, however, that this last reaction may be limited since the Fe^{3+} may form complexes with TBH, leading to a slight increase in the pollutant removal, as already noted by Gozzi et al. (2017) [8]. On the other hand a greater amount of catalyst does not mean an increase in reaction 3, in many cases of Fe^{2+} in the solution can become a scavenger of $^{\bullet}OH$ [15, 46], indeed the best amount of catalyst found was 0.1 mmol L^{-1} of Fe^{2+} (data not shown).

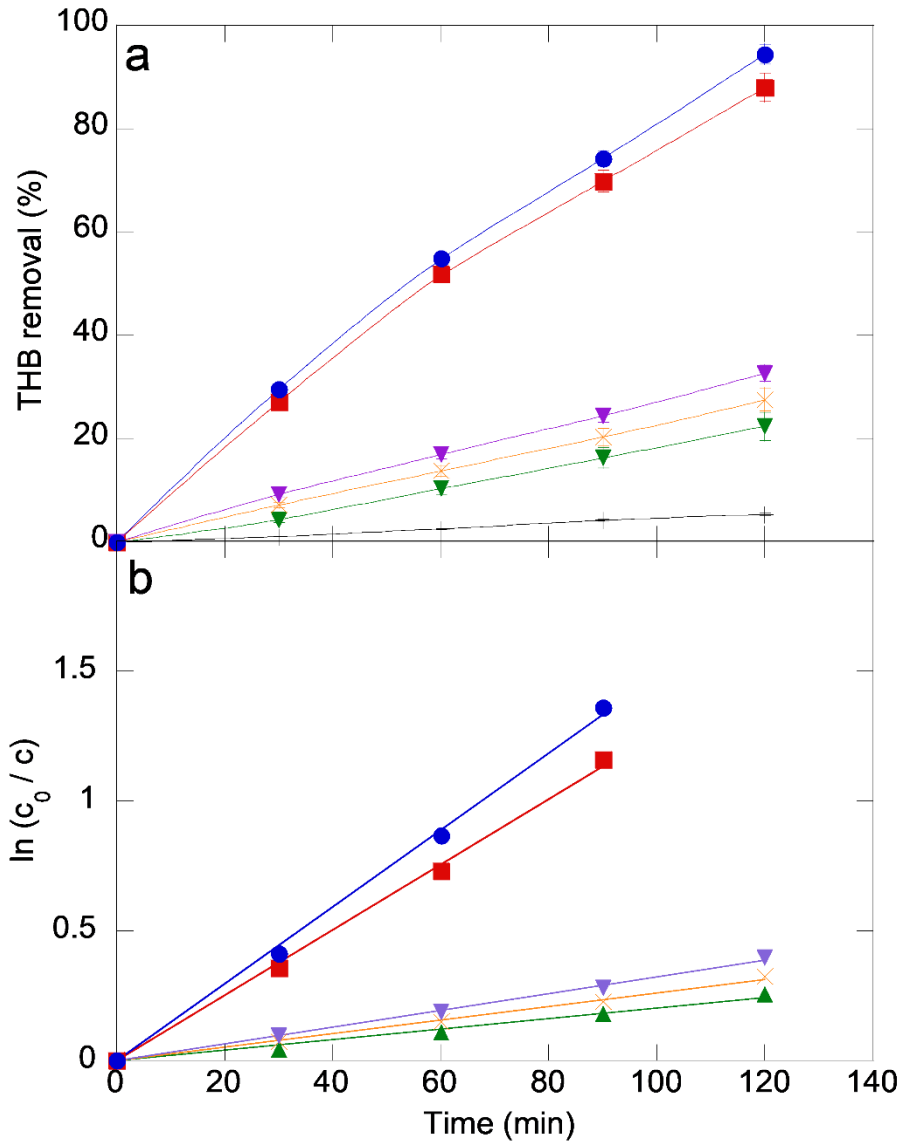

Figure 4. (a) TBH removal and (b) kinetic analysis based on pseudo-first order reaction over time under different EAOPs using 0.1 mol L^{-1} K_2SO_4 at pH = 3.0. EAOPs: (▼) AO, (✕) AO-H_2O_2O, (▼) EF, (■) AO-H_2O_2/UVC and (●) PEF.

Herbicides are commonly regarded as photo-stable compounds. The high degradation kinetics of TBH observed in the AO-H_2O_2/UVC and PEF processes can be attributed to the synergistic effect of UV-C light which promotes the extra generation of $^{\bullet}OH$ in the bulk solution through the photolysis of H_2O_2 (Eq. 11). As can be noted in Fig. 4a, when applied solely, the UVC light does not have great potential for TBH

276 removal (~5.3%); the effect of UVC light is boosted by the addition of H_2O_2 to the
277 system (with 87.9% and 94.5%, for AO-H_2O_2/UVC and PEF processes, respectively).

278 $$H_2O_2 + h\nu \rightarrow 2\ \bullet OH \quad \text{(Eq.11)}$$

279 Apart from the analyses involving the determination of TBH and TOC removal,
280 the figures of merit, including the electrical energy per order (E/EO) (Eq. 12) and
281 mineralization current efficiency (MCE) (Eq. 13), were determined in order to have a
282 better understanding of the viability of the different processes investigated in this study.
283 See equations 12 and 13 below:

284 $$E/EO(kWh\ m^{-3} order^{-1}) = \frac{6.39\times10^{-4}(P_{cell}+P_{lamp})}{V_s k_1} \quad \text{(Eq.12)}$$

285 where 6.39×10^{-4} is a conversion factor (1 h/3600 s/0.4343), P_{cell} and P_{lamp} are
286 the average power of the electrochemical cell and UVC lamp (this is calculated only for
287 the photo-assisted processes), respectively, and k_1 is the pseudo-first order rate constant
288 (s^{-1}) [46,52].

289 $$MCE\ (\%) = \frac{nFVs\Delta(TOC)_{exp}}{4.32\times10^{7}\ m\ I\ t} \times 100 \quad \text{(Eq.13)}$$

290 where F is faraday constant (96,487 C mol^{1}), 4.32×10^{7} is the conversion factor
291 (3,600 s h^{-1} × 12,000 mg C mol^{-1}), Vs corresponds to the treated volume of the solution
292 (L), m is the number of carbon atoms of TBH molecule (m = 9), n is the number of
293 theoretical electrons transferred considering the total mineralization of TBH by equation
294 14 (see below), I is the current (A), and t is the electrolysis time (h) [8].

295 $$C_9H_{16}N_4OS + 33\ H_2O \rightarrow 9CO_2 + 4NO_3^- + SO_4^{2-} + 82\ H^+ + 76\ e^- \quad \text{(Eq.14)}$$

296 As can be observed in Figure 5b, there is a reverse trend between TOC removal and
297 E/EO; higher TOC removal corresponded to lower E/EO. The AO, AO-H_2O_2 and EF
298 processes recorded E/EO values of 143.9, 121.5 and 106.8 kWh m^{-3} $order^{-1}$,
299 respectively, with current efficiencies ranging from 4.2 to 5.3%. The photo-assisted

300 processes recorded E/EO values of approximately 45 kWh m^{-3} $order^{-1}$, with current
301 efficiencies ranging from 16.5% to 17.9% for AO-H_2O_2/UVC and PEF, respectively.

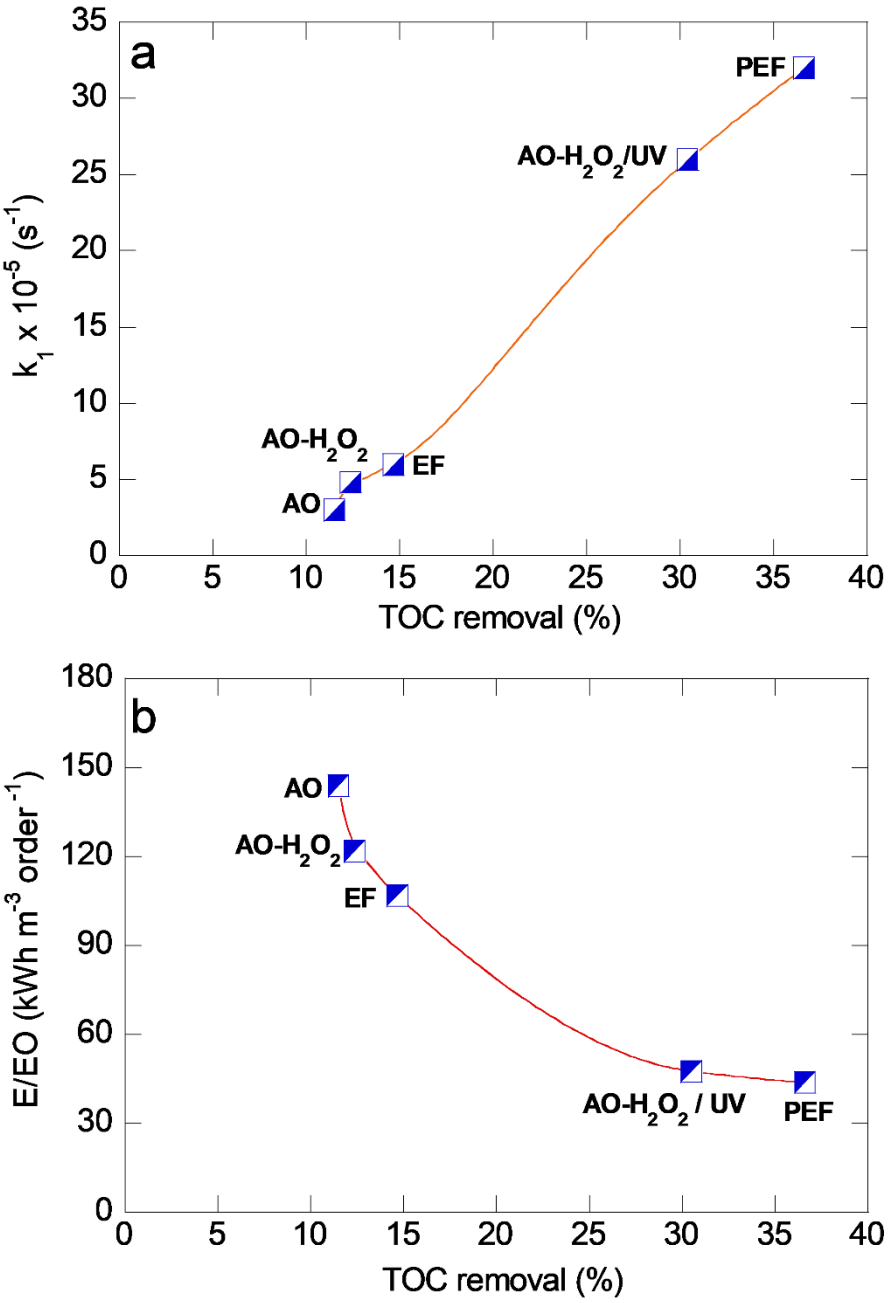

302

303 **Figure 5.** (a) Kinetic analysis and (b) energy electrical per order *vs.* TOC removal for
304 the treatment of 100 mg L^{-1} TBH using a flow-by reactor at pH 3.0, with temperature of
305 25 ºC in 0.1 mol L^{-1} K_2SO_4 and current density of 75 mA cm^{-2} under different EAOPs.

Based on these results, the AO-H_2O_2/UVC and PEF processes were found to be the most suitable techniques for the treatment of solutions containing TBH. Nevertheless, PEF was found to have some non-negligible shortcomings; the process requires the strict application of pH 3.0 and may lead to the formation of Fe(III)-TBH complex. In this sense, AO-H_2O_2/UVC is found to be remarkably outstanding in the sense that it can be used under a wide pH range. Thus, the AO-H_2O_2/UVC process was evaluated under a treatment period of 360 min (Fig. 6); the process resulted in an almost total mineralization (~95%) of TBH. The CE of mineralization (MCE) varied from 30% to 16%; this decrease in MCE (from 30% to 16%) can be justified by the appearance of recalcitrant substances throughout the process which were found to be more difficult to eliminate than the initial compound [53].

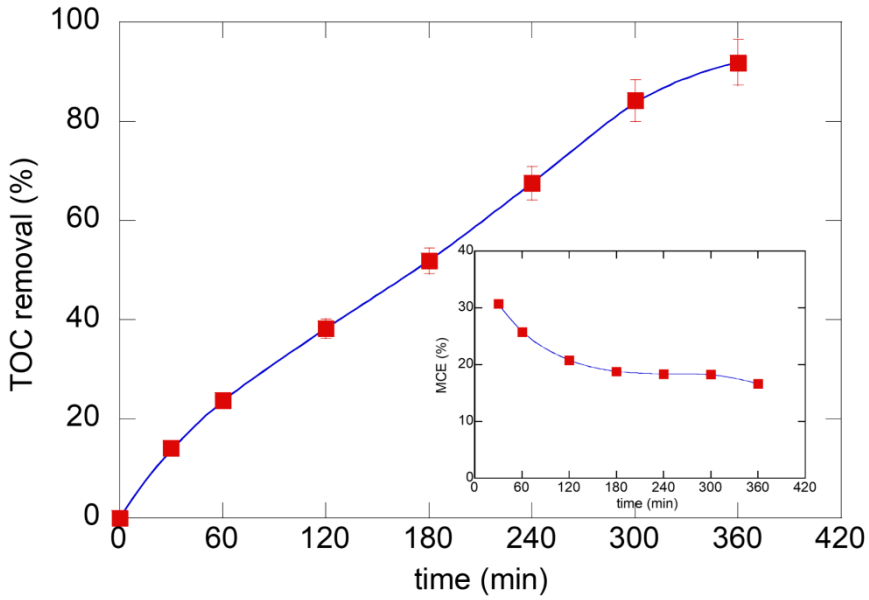

Figure 6. TOC removal *vs.* electrolysis time for the treatment of 100 mg L^{-1} of TBH in a flow-by reactor at pH 3.0, with temperature of 25 ºC, using 0.1 mol L^{-1} K_2SO_4 and current density (*j*) of 75 mA cm^{-2} under AO-H_2O_2/UVC. Inset: Current efficiency over time.

An investigation was also conducted regarding the conversion of initial S and N present in the TBH molecule to inorganic species, such as SO_4^{2-} and NO_3^-. The conversion process yielded SO_4^{2-} concentration of 37.5 mg L^{-1}; this concentration was related to the almost complete conversion of the initial S (14.1 mg L^{-1}) to SO_4^{2-}. With regard to the nitrogenated species (N), a final concentration of 43.3 mg L^{-1} NO_3^- ions (~10.5 mg L^{-1} N-NO_3^-) was obtained; this amount corresponded to 42.7 % of the initial N content (24.6 mg L^{-1}). Other nitrogenated species like NO_2^- and NH_4^+ were not detected; this shows that about 57.3 % of the initial N was lost from the solution in the form of N-volatile species, such as N_2 and NO_x [8,18].

3.3 TBH treatment in real urban wastewater

The water matrix plays an influential role on the efficiency of electrochemical technologies. To further investigate the feasibility of EAOPs, real wastewater containing 100 mg L^{-1} TBH was subjected to treatment in a flow-by reactor using the AO-H_2O_2/UVC technique. Fig 7a shows total TBH removal after 240 min of electrolysis under the application of pH 3.0 and current density of 75 mA cm^{-2}. Under the treatment with real wastewater, the k_1 value recorded a 1.7-fold decrease compared to the treatment with synthetic wastewater ($2.60x10^{-4}$ s^{-1} → $1.55x10^{-4}$ s^{-1}) and E/EO of 54 kWh m^{-3} $order^{-1}$. It is worth noting that the actual effluent had approximately 10 mg L^{-1} of natural organic matter (NOM) in its initial composition due to the presence of some acids such as humic and fulvic acids. Reports in the literature have shown that NOM may act as scavenger of $^{\bullet}$OH radicals [48]. Apart from NOM, the Cl^- present in the water matrix can affect the performance of the system, since the species can be oxidized into active chlorine species (HClO (E^o = 1.49 V|SHE) is the predominant oxidant at pH 3.0) on the BDD surface based on the reactions in equations 15 and 16 [54–56]. Thus, one needs to bear in mind that in real matrices the $^{\bullet}$OH radicals are not

the only oxidants responsible for the removal of TBH, active chlorine species also play a role in the treatment process.

$$2Cl^- \rightarrow Cl_2 + 2e^- \quad \text{(Eq.15)}$$

$$Cl_2 + H_2O \leftrightarrows HClO + Cl^- + H^+ \quad \text{(Eq.16)}$$

When it comes to complex water matrices, one cannot consider the rate of degradation as the only parameter for evaluating the effectiveness of electrochemical techniques. TOC can be useful for analyzing the mineralization of recalcitrant compounds. Fig 7b shows that approximately 78% of the initial organic matter (58 mg L^{-1} TOC, including NOM and TBH) was mineralized at the end of 360 min of treatment. This result points to a relatively lower rate of mineralization and MCE compared to the result obtained from the experiment conducted using synthetic wastewater. The presence of chloride species can improve the efficiency of the system by increasing the number of oxidants in the medium – active chlorine. However, an excess of chloride in the system may act as a scavenger of hydroxyl radicals or promote the formation of hazardous organochlorine compounds.

The chloro oxyanions and inorganic nitrogenous compounds were also monitored in this study; the results are shown in Fig 7c. A complete ammonium removal was observed at the end of the treatment process. Indeed, NH_4^+ can react with active chlorine species, leading to the formation of N_2 gas [54]. For the NO_3^-, a maximum accumulation of 21.3 mg L^{-1} was observed; and part of this compound was reduced to NO_2^- - with concentration of approximately 1.20 mg L^{-1} [57]. Active chlorine species can be oxidized to chlorite (ClO_2^-), chlorate (ClO_3^-) and perchlorate (ClO_4^-) [19]. Final concentrations of 7.30 mg L^{-1} and 3.60 mg L^{-1} we detect for ClO_2^- and ClO_3^-,

370 respectively.

371

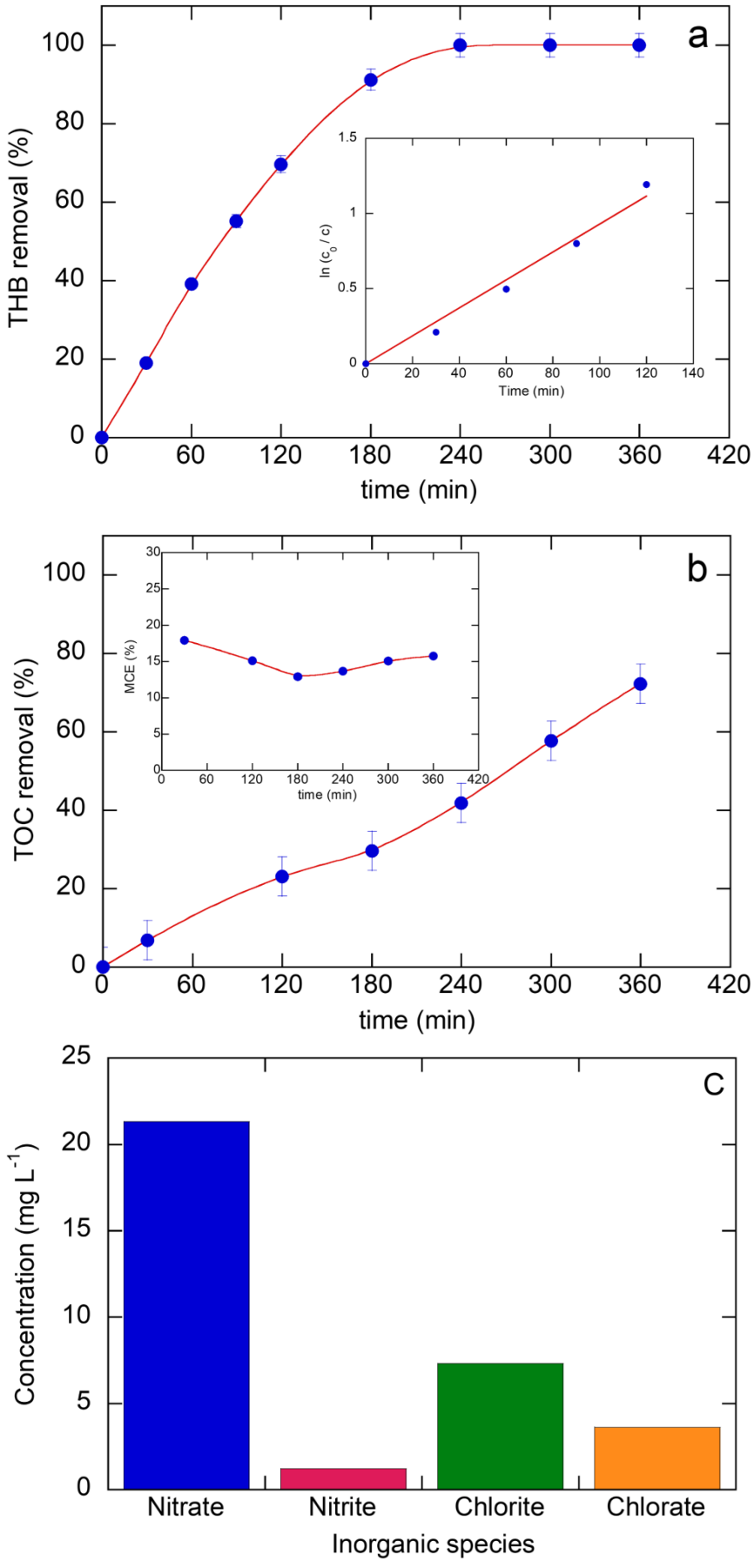

372 **Figure 7.** Removal *vs.* electrolysis time for the treatment of 100 mg L^{-1} of TBH in

373 urban real wastewater using a flow-by reactor at pH 3.0, with temperature of 25 ºC and
374 current density *(j)* of 75 mA cm^{-2} via AO-H_2O_2/UVC. (a) TBH removal. Inset: Kinetic
375 analysis based on pseudo-first order reaction. (b) TOC removal. Inset: Percentage
376 current efficiency. (c) Inorganic species identified at the end of the process.

377 **4 Conclusions**

378 The present work studied the degradation of TBH in both synthetic and real
379 urban wastewater using EAOPs-H_2O_2 with a flow-by reactor. Based on the results
380 obtained, the maximum amount of H_2O_2 electrogenerated was 540.8 mg L^{-1} at 75 mA
381 cm^{-2}; these conditions were applied in the degradation tests. AO and AO-H_2O_2
382 processes demonstrated low efficiency in terms of TBH removal (22.4-27.5%).
383 Electrochemical Fenton-based processes presented some non-negligible shortcomings
384 related to the formation of Fe(III)-TBH complexes. The AO-H_2O_2/UVC process was
385 found to be the most effective technique for TBH removal; this technique presented fast
386 kinetic degradation, high mineralization rate (~95%) and a great degree of versatility
387 once it can be applied under a wide pH range. Furthermore, the application of the AO-
388 H_2O_2/UVC process promoted a 100% satisfactory removal of TBH from real urban
389 wastewater; nonetheless, the formation of organochlorine compounds in this process
390 undermined the overall mineralization process. Based on the findings of this study, the
391 electrochemical treatment processes tested here can be considered highly competitive
392 for application toward the treatment of compounds of interest in real matrices in the
393 near future.
394
395

Acknowledgements

The authors acknowledge the financial support provided by the following Brazilian funding agencies: Brazilian National Council for Scientific and Technological Development - CNPq (grant #465571/2014-0, #302874/2017-8 and #427452/2018-0), São Paulo Research Foundation (FAPESP – grants #2014/50945-4, #2017/23464-3, #2016/25831-0, # 2016/19612-4, #2017/10118-0, #2019/20634-0 and #2019/04421-7), and the Coordenação de Aperfeiçoamento de Pessoal de Nível Superior (CAPES – Finance Code 001).

References

[1] FOOD AND AGRICULTURE ORGANIZATION OF UNITED NATIONS, FOOD Agric. Organ. UNITED NATIONS. Top List Ctries. - 2000 a 2018. (2020). http://www.fao.org/faostat/en/#data/RP/visualize (accessed February 6, 2020).

[2] R.A. la Cruz, G.M. de Oliveira, L.B. de Carvalho, M.F. das G.F. da Silva, Herbicide Resistance in Brazil: Status, Impacts, and Future Challenges, IntechOpen. (2020) 13. doi:10.5772/intechopen.91236.

[3] T.A. Unger, Tebuthiuron, Pestic. Synth. Handb. (1996) 618–619. doi:10.1016/b978-081551401-5.50477-9.

[4] A.T. Faria, M.F. Souza, A.B. Rocha de Jesus Passos, A.A. da Silva, D.V. Silva, J.C. Zanuncio, P.R.R. Rocha, Tebuthiuron leaching in three Brazilian soils as affected by soil pH, Environ. Earth Sci. 77 (2018) 214. doi:10.1007/s12665-018-7285-x.

[5] C.S. Machado, R.I.S. Alves, B.M. Fregonesi, K.A.A. Tonani, B.S. Martinis, J. Sierra, M. Nadal, J.L. Domingo, S. Segura-, Chemical contamination of water and sediments in the Pardo River , Procedia Eng. 162 (2016) 230–237. doi:10.1016/j.proeng.2016.11.046.

[6] Y. Qian, H. Matsumoto, X. Liu, S. Li, X. Liang, Y. Liu, G. Zhu, M. Wang,

Dissipation, occurrence and risk assessment of a phenylurea herbicide tebuthiuron in sugarcane and aquatic ecosystems in South China, Environ. Pollut. 227 (2017) 389–396. doi:10.1016/j.envpol.2017.04.082.

[7] R.A. Dam, C. Camilleri, P. Bayliss, S.J. Markich, Human and Ecological Risk Assessment Ecological Risk Assessment of Tebuthiuron Following Application on Tropical Australian Wetlands Ecological Risk Assessment of Tebuthiuron Following, 7039 (2010). doi:10.1080/10807030490887140.

[8] F. Gozzi, I. Sirés, S.C. de Oliveira, A. Machulek, E. Brillas, Influence of chelation on the Fenton-based electrochemical degradation of herbicide tebuthiuron, Chemosphere. 199 (2018) 709–717. doi:10.1016/j.chemosphere.2018.02.060.

[9] A. Thiam, I. Sirés, R. Salazar, E. Brillas, On the performance of electrocatalytic anodes for photoelectro-Fenton treatment of synthetic solutions and real water spiked with the herbicide chloramben, J. Environ. Manage. 224 (2018) 340–349. doi:10.1016/j.jenvman.2018.07.065.

[10] M.P. Rosa Barbosa, N.S. Lima, D.B. de Matos, R.J. Alves Felisardo, G.N. Santos, G.R. Salazar-Banda, E.B. Cavalcanti, Degradation of pesticide mixture by electro-Fenton in filter-press reactor, J. Water Process Eng. 25 (2018) 222–235. doi:10.1016/j.jwpe.2018.08.008.

[11] A. Fdez-Sanromán, V. Acevedo-García, M. Pazos, M.Á. Sanromán, E. Rosales, Iron-doped cathodes for electro-Fenton implementation: Application for pymetrozine degradation, Electrochim. Acta. 338 (2020) 135768. doi:10.1016/j.electacta.2020.135768.

[12] C.M. Dominguez, N. Oturan, A. Romero, A. Santos, M.A. Oturan, Removal of lindane wastes by advanced electrochemical oxidation, Chemosphere. 202 (2018) 400–409. doi:10.1016/j.chemosphere.2018.03.124.

[13] P.A. Diaw, N. Oturan, M.D.G. Seye, A. Coly, A. Tine, J.J. Aaron, M.A. Oturan, Oxidative degradation and mineralization of the phenylurea herbicide fluometuron in aqueous media by the electro-Fenton process, Sep. Purif. Technol. 186 (2017) 197–206. doi:10.1016/j.seppur.2017.06.005.

[14] D.R.V. Guelfi, Z. Ye, F. Gozzi, S.C. de Oliveira, A. Machulek Junior, E. Brillas,

I. Sirés, Ensuring the overall combustion of herbicide metribuzin by electrochemical advanced oxidation processes. Study of operation variables, kinetics and degradation routes, Sep. Purif. Technol. 211 (2019) 637–645. doi:10.1016/j.seppur.2018.10.029.

[15] E. Brillas, A review on the photoelectro-Fenton process as efficient electrochemical advanced oxidation for wastewater remediation. Treatment with UV light, sunlight, and coupling with conventional and other photo-assisted advanced technologies, Chemosphere. 250 (2020) 126198. doi:10.1016/j.chemosphere.2020.126198.

[16] F.C. Moreira, R.A.R. Boaventura, E. Brillas, V.J.P. Vilar, Electrochemical advanced oxidation processes: A review on their application to synthetic and real wastewaters, Appl. Catal. B Environ. 202 (2017) 217–261. doi:10.1016/j.apcatb.2016.08.037.

[17] I. Sirés, E. Brillas, M.A. Oturan, M.A. Rodrigo, M. Panizza, Electrochemical advanced oxidation processes: Today and tomorrow. A review, Environ. Sci. Pollut. Res. 21 (2014) 8336–8367. doi:10.1007/s11356-014-2783-1.

[18] A. Phetrak, P. Westerhoff, S. Garcia-Segura, Low energy electrochemical oxidation efficiently oxidizes a common textile dye used in Thailand, J. Electroanal. Chem. 871 (2020) 114301. doi:10.1016/j.jelechem.2020.114301.

[19] M. Panizza, G. Cerisola, Direct and mediated anodic oxidation of organic pollutants, Chem. Rev. 109 (2009) 6541–6569. doi:10.1021/cr9001319.

[20] S. Garcia-Segura, J.D. Ocon, M.N. Chong, Electrochemical oxidation remediation of real wastewater effluents — A review, Process Saf. Environ. Prot. 113 (2018) 48–67. doi:10.1016/j.psep.2017.09.014.

[21] A.J. dos Santos, S. Garcia-Segura, S. Dosta, I.G. Cano, C.A. Martínez-Huitle, E. Brillas, A ceramic electrode of ZrO2-Y2O3 for the generation of oxidant species in anodic oxidation. Assessment of the treatment of Acid Blue 29 dye in sulfate and chloride media, Sep. Purif. Technol. 228 (2019) 115747. doi:10.1016/j.seppur.2019.115747.

[22] C.A. Martínez-Huitle, E. Brillas, Decontamination of wastewaters containing synthetic organic dyes by electrochemical methods: A general review, Appl.

Catal. B Environ. 87 (2009) 105–145. doi:10.1016/j.apcatb.2008.09.017.

[23] R. Dewil, D. Mantzavinos, I. Poulios, M.A. Rodrigo, New perspectives for Advanced Oxidation Processes, J. Environ. Manage. 195 (2017) 93–99. doi:10.1016/j.jenvman.2017.04.010.

[24] V.B. Lima, L.A. Goulart, R.S. Rocha, J.R. Steter, M.R.V. Lanza, Degradation of antibiotic ciprofloxacin by different AOP systems using electrochemically generated hydrogen peroxide, Chemosphere. 247 (2020) 125807. doi:10.1016/j.chemosphere.2019.125807.

[25] A.S. Fajardo, A.J. dos Santos, E.C.T. de Araújo Costa, D.R. da Silva, C.A. Martínez-Huitle, Effect of anodic materials on solar photoelectro-Fenton process using a diazo dye as a model contaminant, Chemosphere. 225 (2019) 880–889. doi:10.1016/j.chemosphere.2019.03.071.

[26] M.S. Kronka, F.L. Silva, A.S. Martins, M.O. Almeida, K.M. Honório, M.R. V. Lanza, Tailoring the ORR selectivity for H 2 O 2 electrogeneration by modification of Printex L6 carbon with 1,4-naphthoquinone: a theoretical, experimental and environmental application study , Mater. Adv. (2020) 1318–1329. doi:10.1039/d0ma00290a.

[27] E. Brillas, I. Sirés, M.A. Oturan, Electro-Fenton process and related electrochemical technologies based on Fenton's reaction chemistry., Chem. Rev. 109 (2009) 6570–631. doi:10.1021/cr900136g.

[28] A.J. dos Santos, C.A. Martínez-Huitle, I. Sirés, E. Brillas, Use of Pt and Boron-Doped Diamond Anodes in the Electrochemical Advanced Oxidation of Ponceau SS Diazo Dye in Acidic Sulfate Medium, ChemElectroChem. 5 (2018) 685–693. doi:10.1002/celc.201701238.

[29] W. Wang, X. Lu, P. Su, Y. Li, J. Cai, Q. Zhang, M. Zhou, O. Arotiba, Enhancement of hydrogen peroxide production by electrochemical reduction of oxygen on carbon nanotubes modified with fluorine, Chemosphere. 259 (2020) 127423. doi:10.1016/j.chemosphere.2020.127423.

[30] C. Trellu, Y. Péchaud, N. Oturan, E. Mousset, D. Huguenot, E.D. van Hullebusch, G. Esposito, M.A. Oturan, Comparative study on the removal of humic acids from drinking water by anodic oxidation and electro-Fenton

processes: Mineralization efficiency and modelling, Appl. Catal. B Environ. 194 (2016) 32–41. doi:10.1016/j.apcatb.2016.04.039.

[31] J.F. Carneiro, F.L. Silva, A.S. Martins, R.M.P. Dias, G.M. Titato, Á.J. Santos-Neto, R. Bertazzoli, M.R.V. Lanza, Simultaneous degradation of hexazinone and diuron using ZrO2-nanostructured gas diffusion electrode, Chem. Eng. J. 351 (2018) 650–659. doi:10.1016/j.cej.2018.06.122.

[32] P. Jorge Marques Cordeiro-Junior, M. Schiavon Kronka, L. Athie Goulart, N. Carolina Veríssimo, L. Helena Mascaro, M. Coelho dos Santos, R. Bertazzoli, M. Roberto de Vasconcelos Lanza, Catalysis of oxygen reduction reaction for H2O2 electrogeneration: The impact of different conductive carbon matrices and their physicochemical properties, J. Catal. 392 (2020) 56–68. doi:10.1016/j.jcat.2020.09.020.

[33] A.R. Khataee, M. Safarpour, M. Zarei, S. Aber, Electrochemical generation of H2O2 using immobilized carbon nanotubes on graphite electrode fed with air: Investigation of operational parameters, J. Electroanal. Chem. 659 (2011) 63–68. doi:10.1016/j.jelechem.2011.05.002.

[34] A. Xu, E. Brillas, W. Han, L. Wang, I. Sirés, On the positive effect of UVC light during the removal of benzothiazoles by photoelectro-Fenton with UVA light, Appl. Catal. B Environ. 259 (2019) 118127. doi:10.1016/j.apcatb.2019.118127.

[35] Y. Zhang, S. Zuo, M. Zhou, L. Liang, G. Ren, Removal of tetracycline by coupling of flow-through electro-Fenton and in-situ regenerative active carbon felt adsorption, Chem. Eng. J. 335 (2018) 685–692. doi:10.1016/j.cej.2017.11.012.

[36] A.J. dos Santos, E.C.T. de A. Costa, D.R. da Silva, S. Garcia-Segura, C.A. Martínez-Huitle, Electrochemical advanced oxidation processes as decentralized water treatment technologies to remediate domestic washing machine effluents, Environ. Sci. Pollut. Res. 25 (2018) 7002–7011. doi:10.1007/s11356-017-1039-2.

[37] G.F. Pereira, B.F. Silva, R. V. Oliveira, D.A.C. Coledam, J.M. Aquino, R.C. Rocha-Filho, N. Bocchi, S.R. Biaggio, Comparative electrochemical degradation of the herbicide tebuthiuron using a flow cell with a boron-doped diamond anode

548 and identifying degradation intermediates, Electrochim. Acta. 247 (2017) 860–
549 870. doi:10.1016/j.electacta.2017.07.054.

550 [38] A. Klančar, J. Trontelj, A. Kristl, A. Meglič, T. Rozina, M.Z. Justin, R. Roškar,
551 An advanced oxidation process for wastewater treatment to reduce the ecological
552 burden from pharmacotherapy and the agricultural use of pesticides, Ecol. Eng.
553 97 (2016) 186–195. doi:10.1016/j.ecoleng.2016.09.010.

554 [39] I.J.S. Montes, B.F. Silva, J.M. Aquino, Applied Catalysis B : Environmental On
555 the performance of a hybrid process to mineralize the herbicide tebuthiuron using
556 a DSA ® anode and UVC light : A mechanistic study, 200 (2017) 237–245.
557 doi:10.1016/j.apcatb.2016.07.003.

558 [40] G. Pliego, J.A. Zazo, P. Garcia-Muñoz, M. Munoz, J.A. Casas, J.J. Rodriguez,
559 Trends in the Intensification of the Fenton Process for Wastewater Treatment: An
560 Overview, Crit. Rev. Environ. Sci. Technol. 45 (2015) 2611–2692.
561 doi:10.1080/10643389.2015.1025646.

562 [41] S. Garcia-Segura, A.B. Nienhauser, A.S. Fajardo, R. Bansal, C.L. Coonrod, J.D.
563 Fortner, M. Marcos-Hernández, T. Rogers, D. Villagran, M.S. Wong, P.
564 Westerhoff, Disparities between experimental and environmental conditions:
565 Research steps toward making electrochemical water treatment a reality, Curr.
566 Opin. Electrochem. 22 (2020) 9–16. doi:10.1016/j.coelec.2020.03.001.

567 [42] A.J. Dos Santos, M.D. De Lima, D.R. Da Silva, S. Garcia-Segura, C.A.
568 Martínez-Huitle, Influence of the water hardness on the performance of electro-
569 Fenton approach: Decolorization and mineralization of Eriochrome Black T,
570 Electrochim. Acta. 208 (2016) 156–163. doi:10.1016/j.electacta.2016.05.015.

571 [43] R.M. Reis, A.A.G.F. Beati, R.S. Rocha, M.H.M.T. Assumpção, M.C. Santos, R.
572 Bertazzoli, M.R. V Lanza, Use of gas diffusion electrode for the in situ
573 generation of hydrogen peroxide in an electrochemical flow-by reactor, Ind. Eng.
574 Chem. Res. 51 (2012) 649–654. doi:10.1021/ie201317u.

575 [44] J. Moreira, V. Bocalon Lima, L. Athie Goulart, M.R.V. Lanza, Electrosynthesis
576 of hydrogen peroxide using modified gas diffusion electrodes (MGDE) for
577 environmental applications: Quinones and azo compounds employed as redox
578 modifiers, Appl. Catal. B Environ. 248 (2019) 95–107.

579 doi:10.1016/j.apcatb.2019.01.071.

580 [45] W. Zhou, X. Meng, J. Gao, A.N. Alshawabkeh, Hydrogen peroxide generation
581 from O 2 electroreduction for environmental remediation: A state-of-the-art
582 review, Chemosphere. 225 (2019) 588–607.
583 doi:10.1016/j.chemosphere.2019.03.042.

584 [46] G. V. Fortunato, M.S. Kronka, A.J. dos Santos, M. Ledendecker, M.R.V. Lanza,
585 Low Pd loadings onto Printex L6: Synthesis, characterization and performance
586 towards H2O2 generation for electrochemical water treatment technologies,
587 Chemosphere. 259 (2020) 127523. doi:10.1016/j.chemosphere.2020.127523.

588 [47] W.R.P. Barros, T. Ereno, A.C. Tavares, M.R.V. Lanza, In Situ Electrochemical
589 Generation of Hydrogen Peroxide in Alkaline Aqueous Solution by using an
590 Unmodified Gas Diffusion Electrode, ChemElectroChem. 2 (2015) 714–719.
591 doi:10.1002/celc.201402426.

592 [48] A.J. dos Santos, P.L. Cabot, E. Brillas, I. Sirés, A comprehensive study on the
593 electrochemical advanced oxidation of antihypertensive captopril in different
594 cells and aqueous matrices, Appl. Catal. B Environ. 277 (2020) 119240.
595 doi:10.1016/j.apcatb.2020.119240.

596 [49] J.C. Murillo-Sierra, I. Sirés, E. Brillas, E.J. Ruiz-Ruiz, A. Hernández-Ramírez,
597 Advanced oxidation of real sulfamethoxazole + trimethoprim formulations using
598 different anodes and electrolytes, Chemosphere. 192 (2018) 225–233.
599 doi:10.1016/j.chemosphere.2017.10.136.

600 [50] L. Ma, M. Zhou, G. Ren, W. Yang, L. Liang, A highly energy-efficient flow-
601 through electro-Fenton process for organic pollutants degradation, Electrochim.
602 Acta. 200 (2016) 222–230. doi:10.1016/j.electacta.2016.03.181.

603 [51] N. Oturan, S.O. Ganiyu, S. Raffy, M.A. Oturan, Sub-stoichiometric titanium
604 oxide as a new anode material for electro-Fenton process: Application to
605 electrocatalytic destruction of antibiotic amoxicillin, Appl. Catal. B Environ. 217
606 (2017) 214–223. doi:10.1016/j.apcatb.2017.05.062.

607 [52] R. Montenegro-Ayo, J.C. Morales-Gomero, H. Alarcon, S. Cotillas, P.
608 Westerhoff, S. Garcia-Segura, Scaling up photoelectrocatalytic reactors: A TiO2
609 nanotube-coated disc compound reactor effectively degrades acetaminophen,

610 Water (Switzerland). 11 (2019) 1–14. doi:10.3390/w11122522.

611 [53] C.M. Dominguez, N. Oturan, A. Romero, A. Santos, M.A. Oturan, Lindane
612 degradation by electrooxidation process: Effect of electrode materials on
613 oxidation and mineralization kinetics, Water Res. 135 (2018) 220–230.
614 doi:10.1016/j.watres.2018.02.037.

615 [54] S. Garcia-Segura, E. Mostafa, H. Baltruschat, Electrogeneration of inorganic
616 chloramines on boron-doped diamond anodes during electrochemical oxidation
617 of ammonium chloride, urea and synthetic urine matrix, Water Res. 160 (2019)
618 107–117. doi:10.1016/j.watres.2019.05.046.

619 [55] A. Jhones dos Santos, I. Sirés, E. Brillas, Removal of bisphenol A from acidic
620 sulfate medium and urban wastewater using persulfate activated with
621 electroregenerated Fe2+, Chemosphere. 263 (2021) 1–11.
622 doi:10.1016/j.chemosphere.2020.128271.

623 [56] E. Mousset, L. Quackenbush, C. Schondek, A. Gerardin-Vergne, S. Pontvianne,
624 S. Kmiotek, M.N. Pons, Effect of homogeneous Fenton combined with electron
625 transfer on the fate of inorganic chlorinated species in synthetic and reclaimed
626 municipal wastewater, Electrochim. Acta. 334 (2020).
627 doi:10.1016/j.electacta.2019.135608.

628 [57] S. Garcia-Segura, M. Lanzarini-Lopes, K. Hristovski, P. Westerhoff,
629 Electrocatalytic reduction of nitrate: Fundamentals to full-scale water treatment
630 applications, Appl. Catal. B Environ. 236 (2018) 546–568.
631 doi:10.1016/j.apcatb.2018.05.041.

632

633